Temperature-dependent regulation of *Arabidopsis thaliana* growth and development by *LSM7*

Sarah Muniz Nardeli[1]; Vasiliki Zacharaki[1]; Nelson Rojas-Murcia[1]; Silvio Collani[1]; Kai Wang[2,4]; Martin Bayer[2,5]; Markus Schmid[1,3*]; Daniela Goretti[1]

[1]Umeå Plant Science Centre, Department of Plant Physiology, Umeå University, SE-90187 Umea, Sweden
[2]Max Planck Institute for Developmental Biology, Department of Cell Biology, 72076 Tuebingen, Germany
[3]Department of Plant Biology, Linnean Center for Plant Biology, Swedish University of Agricultural Sciences, S-75007 Uppsala, Sweden
[4]Present address: Oil Crops Research Institute of the Chinese Academy of Agricultural Sciences, 430062 Wuhan, People's Republic of China
[5]Present address: University of Tuebingen, Center for Plant Molecular Biology (ZMBP), 72076 Tuebingen, Germany

*corresponding author

Author emails and ORCID:
sarah.nardeli@umu.se (0000-0001-8858-807X)
vasiliki.zacharaki@umu.se (0000-0002-5543-2332)
nelson.rojas@umu.se (0000-0001-6058-6830)
silvio.collani@umu.se (0000-0002-9603-0882)
wangkai20107266@163.com (0000-0002-5370-4170)
martin.bayer@zmbp.uni-tuebingen.de (0000-0001-5806-2253)
markus.schmid@slu.se (0000-0002-0068-2967)
daniela.goretti@umu.se (0000-0003-3996-0204)

Abstract

SM-like (LSM) proteins are highly conserved among eukaryotes. By promoting alternative splicing and modulating RNA levels, LSM proteins are key regulators of plant development and response to environmental signals. Here, we report that *Arabidopsis* LSM7 is essential for embryogenesis, and that downregulation of *LSM7* results in temperature-dependent developmental defects. Performing a comprehensive transcriptome analysis, we observed that *LSM7* modulates flowering, stress-responsive and auxin-related gene expression. Auxin metabolic profiling correlates with our transcriptome analyses and indicates a role of LSM7 in auxin homeostasis and signalling. We propose that LSM7 splicing activity is essential for plant acclimation and survival at different ambient temperatures and that alterations in auxin content are causally linked to the phenotypic defects in the mutant. This study highlights the essential role of LSM proteins in plant development and provides new insights into the molecular and metabolomic aspects underlying plant temperature acclimation.

Keywords

Splicing; mRNA degradation; SM-like; post-transcriptional regulation; RNA-binding proteins, ambient temperature; thermotolerance; abiotic stress; plant development; auxin.

Introduction

Temperature is a critical environmental factor affecting plant development and limiting their geographical distribution. Globally, plants have evolved mechanisms to survive a wide range of climates. However, the capacity of any given plant species to adjust to changes in its environment is usually much more limited. Several studies have shown that severe heat and cold affect plant fitness and processes like seed germination and flowering and the underlying molecular mechanisms have been intensively studied[1]. In contrast, understanding how plants respond to suboptimal but non-stressful ambient temperature changes is lacking despite its obvious importance given climate change.

To adjust to such subtle environmental changes, plants reprogram their transcriptome, which involves regulation at the level of gene expression, RNA processing, and RNA stability. RNA processing, and in particular alternative RNA splicing (AS), is a key mechanism that enables plants to rapidly respond and acclimate to new environmental conditions[2]. mRNA splicing is regulated by the spliceosome, a large ribonucleoprotein machinery, which assembles around heptameric rings of SM and SM-like (LSM) proteins containing U-rich snRNAs (U1, U2, U4, U5, and U6). While the SM ring is best known for its function in RNA splicing, LSM rings have a dual function, depending on their composition. The nuclear-localised heptameric LSM2-8 ring binds to the 3′ end of the spliceosomal snRNA U6[3] and

participates primarily in RNA splicing[4]. In contrast, the LSM1-7 complex participates in mRNA degradation by recognising mRNAs with short poly(A) 3′ ends in the cytoplasm[5]. mRNA degradation is mediated by the nonsense-mediated decay (NMD) surveillance pathway that recognises mRNAs with premature termination codons (PTCs). The PTC-containing mRNAs are generated by nonsense mutations or errors that occur during transcription and splicing, and it eliminates the aberrant transcripts to protect the cell from producing potentially harmful truncated proteins[6]. This coupling of alternative splicing and NMD can be used to co- or post-transcriptionally regulate the level of mRNA[7].

Numerous lines of evidence implicate splicing in plant temperature acclimation[8,9]. However, the underlying molecular mechanisms, and in particular the contribution of core spliceosome components, are still poorly understood. Heat stress experiments showed that high temperature (37°C) affects subcellular localisation of the LSM3A, LSM3B, LSM4, and LSM5 proteins[10]. More extreme heat stress conditions (temperatures above 42°C) require a functional LSM5, whose absence causes miss-splicing of heat shock transcription factors, resulting in seedling lethality[11]. Other studies showed that LSM8 and PCP/SME1 are required for cold (4°C) acclimation[10–12], indicating that (L)SM proteins participate in the acclimation to both extreme heat and cold. Moreover, the core splicing gene *PCP*/*SME1* has also been implicated in the regulation of growth and development in *Arabidopsis thaliana* within the non-stressful ambient temperature range between 16°C to 27°C[13]. Highlighting the importance of RNA processing for proper plant development is the finding that mutations in key splicing genes, including *LSM* genes, often cause embryonic or postembryonic lethality[14]. This property, unfortunately, makes investigating the role of these core splicing genes in response to environmental signals at a later point in growth and development extremely challenging.

The plant hormone auxin is well known for its role in establishing polarity in the plant embryo as well as subsequent embryo development (for review[15]). For example, after the first zygotic division or later at the globular stage, the establishment of directional auxin transport is critical for determining the apical-basal polarity of the embryo[16]. In adult plants, auxin continues to control cell identity and consequently affects diverse processes such as root growth[17], vascular strands and leaf venation[18], and flower development[19]. Auxin biosynthesis, transport, perception, and signalling have also been shown to modulate plant responses to different types of stress, both biotic and abiotic, including temperature[20]. For example, cold (4°C) has been shown to affect the polar distribution of auxin in the root and its accumulation in the root meristem modulates root growth and gravitropism[21]. Importantly, the function of auxin is not limited to responses to cold but numerous studies have implicated auxin biosynthesis and signalling in thermomorphogenesis, the process in which plants elongate their hypocotyl and petioles, decrease the size of their leaf blade and move their leaves upwards to allow efficient airflow for cooling during heat stress[22].

Here we show that LSM7 directly interacts with PCP/SME1, a core component of the spliceosome previously implicated in the regulation of temperature responses in *Arabidopsis*[13]. Not surprisingly for a single-copy gene encoding an essential subunit of the LSM ring, knock-out of *LSM7* by a T-DNA insertion in the coding sequence (*lsm7-1*) resulted in embryo lethality. However, viable homozygous mutant plants could be recovered for a second allele, *lsm7-2,* which carries a T-DNA insertion in the 3' UTR, resulting in a severe reduction in *LSM7* expression. Identification of this strong knock-down allele enabled us for the first time to investigate the function of LSM7 during vegetative and reproductive development. We find that *lsm7*-2 plants are hypersensitive to a warm ambient temperature of 27°C and display a massive alteration of the auxin-related transcriptome and metabolome. Our results provide important insights into the interplay between RNA processing and the regulation of auxin homeostasis in response to changes in ambient temperature, setting the stage for exploring the potential of modulating RNA processing to mitigate the effects of global warming on plant performance.

Results

Embryo and plant development require functional LSM7

Arabidopsis PCP, also known as SME1, is the ortholog of the human core spliceosomal SNRPE and the yeast SME proteins and it is indispensable for normal plant growth and development under cold and cool ambient temperatures[13,23]. In a large-scale protein-protein interaction screen[24], PCP has been shown to directly interact with LSM7, a subunit of the LSM ring encoded by a single copy gene (*AT2G03870*) that has not previously been characterised. Yeast-two-hybrid analysis confirmed that LSM7 indeed interacts with both PCP and its paralog, PCP-like/SME2, and was therefore selected for further analysis (**Supplementary Fig. 1a,b**).

First, we isolated a line bearing a T-DNA insertion in the third intron of the gene (designated as *lsm7-1*) (**Fig. 1a**). More than 100 *lsm7-1* heterozygous (*lsm7-1*+/-) plants were grown on soil, but no homozygous individuals were recovered. In addition, we observed that circa 27% of the ovules checked (n=139) in the siliques of *lsm7-1*+/- plants were aborted. The observed ratio of aborted ovules indicates that a single recessive mutation is the cause of the embryo lethality in the *lsm7-1*-/- mutant. Whole mount analysis of ovules from *lsm7-1*+/- plants showed that 24% (31 out of 130) of the embryos were arrested at the late globular stage **(Fig. 1b)**. In the same siliques, *lsm7-1*+/- and wildtype embryos already reached the bend cotyledon stage **(Fig. 1b)**. We also observed infrequent other aberrations in the *lsm7-1*-/- embryos, such as enlarged suspensor, hypophysis, and defects in the division pattern in the embryo proper **(Fig. 1b)**. Expression of the *LSM7* coding (*pLSM7::cdsLSM7::tLSM7*) or genomic

(*pLSM7::gLSM7::tLSM7*) regions rescued the mutant, confirming that the loss of *LSM7* is the cause of the embryo lethality in *lsm7-1* **(Fig. 1c, Supplementary Fig. 2a)**. It should be noted that although all the randomly chosen T2 transgenic plants eventually resembled wildtype, the margins of the first true leaves were curled upward **(Supplementary Fig. 2b)**, suggesting that the rescue constructs lack certain *cis*-regulatory elements.

Since *lsm7-1* is embryo lethal, a second allele of *LSM7*, designated as *lsm7-2* was characterised. In contrast to *lsm7-1, lsm7-2* is viable and further analysis showed that the T-DNA insertion was inserted in the 3' UTR and not in the last exon as reported in public T-DNA insertion databases (**Fig. 1a**). Given the location of the T-DNA insertion, we assumed that *lsm7-2* might be a knock-down allele. Indeed, we found that *LSM7* expression was significantly reduced in *lsm7-2* compared to wildtype plants **(Fig. 2a**). Although *lsm7-2* is not embryo lethal, it does display pleiotropic defects when grown at 23°C, including a smaller rosette diameter (*lsm7-2*, 3.72±0.44 cm; and Col-0, 7.24±0.47 cm), reduced leaf curvature, irregular leaf margins, and darker colour (**Fig. 2b**). The reduced rosette size of the plants mirrors a smaller shoot apical meristem (**Fig. 2c**). In contrast, the root meristem structure appeared similar to that of wildtype even though the total length of the root is drastically reduced in *lsm7-2* (**Fig. 2d; Supplementary Fig. 3a**). Furthermore, *lsm7-2* flowered earlier than Col-0 (**Fig. 2e; Supplementary Fig. 3b**). We also confirmed by backcrossing *lsm7-2* to Col-0 and analysing the segregation rate in the F2 generation that the *lsm7-2* phenotype is caused by a single recessive mutation. Overall, our results highlight the need for a minimum level of *LSM7* expression to ensure proper embryo and plant development.

***LSM7* is important for plant development across the ambient temperature range**

LSM7 has been shown to interact with PCP, which is hypersensitive to cool ambient temperatures. To test whether LSM7 plays a similar role in temperature response, we recorded the phenotype of *lsm7-2* and Col-0 plants at 16°C and 27°C. Interestingly, in addition to the phenotype described above for *lsm7-2* grown at 23°C (**Fig. 2b**), at 16°C *lsm7-2* flowered much earlier than wildtype plants (**Fig. 2e; Supplementary Fig. 3b**), while reduction in rosette size in *lsm7-2* was comparable between plants grown at 23°C and 16°C. In contrast to 23°C and 16°C, an elevated ambient temperature of 27°C dramatically affected the growth of *lsm7-2*. Plants grew very slowly and up to 82% of seedlings eventually died **(Fig. 2b)**. To confirm that the downregulation of *LSM7* is responsible for the death of the seedlings at 27°C we introduced the *LSM7* genomic and CDS rescue constructs described above into *lsm7-2*. We observed for each construct that multiple independent T1 plants (n>25) grown at 27°C developed into wildtype-like plants able to set seeds (**Fig. 2f; Supplementary Fig. 4a,b**), confirming that *lsm7-2* is causing the phenotype. Given that the phenotype of *lsm7-2* becomes more severe with increasing temperatures, we tested whether *LSM7* expression is modulated

by ambient temperatures. We found that *LSM7* expression was always significantly reduced in *lsm7-2* compared to Col-0 across all temperatures tested (16°C, 23°C, and 27°C) (**Fig. 2a**), letting us hypothesise that other layers of regulation contribute to the temperature-specific function of LSM7. Interestingly, *lsm7-2* seems to be particularly sensitive to elevated ambient temperature but not to PEG-induced osmotic stress and increasing concentrations of NaCl, which significantly reduced root growth in Col-0 but had no additional effect on *lsm7-2* (**Fig. 2g; Supplementary Fig. 3a**). It should be noted, however, that the root of *lsm7-2* is much shorter to begin with. Taken together, our results indicate an essential role for *LSM7* in the response to ambient temperature and especially to warm conditions, highlighting the importance of RNA processing for plant temperature acclimation.

LSM7 is ubiquitously expressed in plants and its protein accumulation is temperature-independent

Since LSM7 protein is essential for plant development, we investigated the expression pattern of the LSM7 protein using a 3xGFP-NLS reporter under the control of the *LSM7* promoter and terminator (*pLSM7::3xGFP-NLS::tLSM7*). The GFP signal became detectable in the suspensor and the embryo proper as early as the preglobular stage (**Fig. 3a**). GFP was expressed evenly in all cells during the late globular and early heart stage, but expression increased in the root and shoot meristem during later stages of embryogenesis (**Fig. 3a**). Enhanced expression of the *LSM7* reporter in the root and shoot meristem was also noticeable in seven-day-old seedlings (**Fig. 3b**). Induction of *LSM7* expression during early stages of embryogenesis is in line with the embryo lethal phenotype of the *lsm7-1* null mutant. Given that the *lsm7-2* mutant is temperature sensitive we prepared a genomic GFP-tagged line (**Fig. 2f**) to test the hypothesis that temperature might affect LSM7 protein accumulation. However, western blot analysis using protein extracts prepared from whole seedlings showed no sign of temperature specific LSM7 protein accumulation (**Fig. 3c**), nor did the subcellular localisation of LSM7-GFP changed significantly (**Fig. 3d**), indicating that *lsm7-2* temperature-dependency is controlled by regulatory mechanisms other than protein stability.

Global effects of *lsm7-2* on the *Arabidopsis* transcriptome

To better understand the effects of *lsm7-2* on the transcriptome in response to changes in ambient temperature a strand-specific RNA-Seq experiment was performed. Seedlings were grown at 23°C for nine days before being shifted to either 16°C or 27°C, and samples were taken 3h and 24h after the shift. Plants maintained at 23°C throughout the course of the experiment served as a control (**Fig. 4a**). Principal component analysis shows that across all the samples the genotype explains most of the variance (31.77%) observed in the data set, followed by temperature (24.58%) **(Fig. 4b)**. Differentially expressed (DE) and differentially

alternatively spliced (DAS) genes were identified by comparing the mutant and wildtype transcriptomes obtained at the three temperatures for each time point **(Fig. 4c; Supplementary Table 1 and 2)**. Not surprisingly given the major effect of the genotype on the transcriptome, we detected a similar number of genes being up- or down-regulated at the three temperatures. Nevertheless, the exposure to high and low temperatures increased the number of DE genes between *lsm7-2* and Col-0 by at least 33.5% and this increase is more pronounced 24h after the shift **(Fig. 4d; Supplementary Table 1**). As expected for a mutant affected in both AS and NMD, we observed more upregulated DAS genes in *lsm7-2* in all conditions tested **(Supplementary Table 2).**

LSM7 regulates the accumulation of flowering-related transcripts in *Arabidopsis*

Since the *lsm7-2* mutant flowers significantly earlier than wildtype when grown at 16°C and 23°C (**Fig. 2e**), we compared the transcriptome profiles of nine-day-old Col-0 and *lsm7-2* seedlings before the temperature shift (0h). We detected 2709 and 2840 genes that were differentially expressed (DE) or differentially alternatively spliced (DAS), respectively, and in total 445 genes that were DE and DAS up- or downwards (**Fig.5a; Supplementary Table 1 and 2**). Gene Ontology (GO) analysis of Biological Processes (BPs) revealed that genes involved in regulating flowering and reproductive development were overrepresented among the DE and DAS genes (**Fig. 5b; Supplementary Table 3**). Consistent with the early flowering of *lsm7-2* (**Fig. 2e**), our analysis showed that *FLOWERING LOCUS T* (*FT*) and *SUPPRESSOR OF OVEREXPRESSION OF CONSTANS* (*SOC1*) were upregulated while their direct repressor *FLOWERING LOCUS C (FLC)* was downregulated (**Fig. 5c**). Expression of *CO* (*CONSTANS)*, an upstream regulator of *FT*, was not changed (**Fig. 5c**). Interestingly, several genes of the autonomous flowering pathway were DAS in *lsm7-2* (**Supplementary Fig. 5a,b**), suggesting that AS or inefficient splicing of these known upstream regulators of *FLC* may contribute to its downregulation in *lsm7-2*, although this hypothesis needs to be further investigated. Taken together, our results suggest that in *lsm7-2* induction of *FT* and *SOC1* occurs independently of *CO* but might require downregulation of the floral repressor *FLC*.

Since LSM7 is a core component of the spliceosome and the NMD pathway, *FLC* downregulation in *lsm7-2* may be due to impaired splicing and subsequent targeted RNA degradation. However, even though RT-qPCR confirmed the down-regulation of *FLC* and *COOLAIR* class II, an antisense transcript implicated in *FLC* regulation, we did not observe any differences in the half-life of the transcripts at *FLC* locus between Col-0 and *lsm7-2* (**Supplementary Fig. 5c-e).** Taken together, our results suggest that *LSM7* is required for correct expression of *FLC*.

Global effects of *lsm7-2* on the temperature-responsive transcriptome

To assess the role of LSM7 in the responses to changes in temperature we performed GO enrichment analysis on genes that were DE 3h (initial response) and 24h (late response) after the shift to 16°C or 27°C (**Supplementary Table 3**). We found that exposure to low ambient temperature had a strong impact on processes such as RNA processing and maturation, ncRNA processing, regulation of translation, and ribosome biogenesis. The initial response to 16°C also included GO categories related to "response to bacteria", with more GO terms related to "biotic stress", "systemic acquired resistance", and "response to salicylic acid" appearing during the late response (24h) to low ambient temperature. In contrast, exposure to high ambient temperature (27°C) had a strong effect on "photosynthetic-related" processes, "response to light" and "temperature" (**Fig. 6; Supplementary Table 3**). Taken together, and not too surprising for a component of the core spliceosome and NMD pathways, our transcriptome analysis indicates that LSM7 participates in the regulation of many different biological processes in the cell, which is in line with the strong pleiotropic phenotype of the *lsm7-2* knock-down mutant.

***lsm7-2* modulates auxin metabolism and homeostasis**

A number of GO categories that stood out in our analysis were those related to auxin as these were overrepresented in all experimental conditions (**Fig. 6; Supplementary Table 3**). In particular, we found many auxin-responsive genes of the *Gretchen Hagen 3* (*GH3*), *Auxin/Indole-3-Acetic Acid* (*Aux/IAA*), *auxin response factor* (*ARF*), and *small auxin up-regulated RNA* (*SAUR*) families to be miss-regulated in *lsm7-2* at 23°C. The degree of misregulation of these gene families was even more pronounced at elevated or cool ambient temperatures (**Fig. 7a**), indicating that *LSM7* plays a critical role in regulating auxin homeostasis and signalling across the entire range of ambient temperature. We, therefore, decided to investigate in more detail if part of the phenotypic defects in *lsm7-2* could be attributed to imbalanced auxin homeostasis or signalling.

Expression of genes involved in auxin biosynthesis was uninformative with some genes being upregulated and others being downregulated in *lsm7-2*, and no clear correlation with temperature (**Supplementary Fig. 6a**). Nevertheless, metabolic analysis revealed significantly elevated levels of the auxin precursors IAN and IAM in *lsm7-2* at all three temperatures whereas free IAA was significantly induced only in mutant plants grown at 23°C (**Supplementary Fig. 6b**), suggesting plants strive to maintain IAA homeostasis, possibly by activating IAA catabolism.

In agreement with this hypothesis, we found that genes encoding GH3 proteins, which are involved in the conjugation of free IAA to amino acids for storage or degradation, were highly overrepresented among the DE and DAS genes in *lsm7-2*. This induction of *GH3s* was

reflected in a significant increase of IAA-Asp, IAA-Glu, and IAA-Ala conjugates in the mutant at all three temperatures (**Fig. 7a,b**). Furthermore, we found that other genes involved in IAA conjugation and catabolism, namely *ILR1*, *DAO2* and *UGT74D1* were also significantly upregulated (**Fig. 7a**), correlating with an increase in oxIAA and oxIAA-Glc in *lsm7-2* at all three temperatures (**Fig. 7b**). Interestingly, we observed an increase of IAA-Glc only after 24h shift to 27°C, which was previously reported under high-temperature condition[25]. Taken together these results indicate that the total pool of auxin is increased in *lsm7-2*. This overaccumulation of auxin is also consistent with the downregulation of the IAA influx genes and the upregulation of IAA efflux genes we observe in *lsm7-2* (**Fig. 7a**), which likely reflects the plant's effort to decrease cellular auxin levels by pumping out IAA.

As auxin metabolism and homeostasis seem to be disturbed in *lsm7-2*, the question arises which auxin signalling genes are misregulated and realise the growth responses observed in the mutant. We found that several *Aux/IAA* genes (16 out of 32) and *ARF* genes (8 out of 23), well-known regulators of the transcriptional response to auxin, were DE in *lsm7-2*. However, the most interesting gene group related to auxin signalling were the *SMALL AUXIN UP-REGULATED RNA* (*SAUR*) genes, which play a central role in the regulation of IAA-induced growth[26]. Of the 79 *SAUR* genes in the *Arabidopsis* genome, 42 were DE, of which 35 were significantly downregulated in *lsm7-2*, especially at elevated ambient temperature (**Fig. 7a)**. Importantly, central heat shock genes (*HSP90.1*, *HSP70.4* and *HSFB2A*) were induced similarly to wildtype plants (**Supplementary Fig. 6c**) when grown at 27°C, suggesting that temperature sensing *per se* in *lsm7-2* is intact. In summary, our combined transcriptomic and metabolomic analysis suggest that LSM7 has a key role in the regulation of auxin homeostasis and signal transduction to ensure proper plant growth and development, in particular at elevated ambient temperatures.

Discussion

Sessile organisms, such as plants, cannot escape adverse environments. Instead, they have evolved intricate mechanisms to monitor their surroundings and to detect and respond to perturbations. A signal that is of particular importance for the coordination of plant growth and development is temperature, which acts on different scales, ranging from the more subtle variations a plant experiences over the course of a day to extreme summer heat and winter cold. While recent years have seen tremendous progress in the understanding of the molecular pathways involved in temperature perception, how these signals actually modulate plant growth and development is less well understood.

Here, we show that LSM7, a core component of the spliceosome and NMD pathway, is essential for *Arabidopsis* development. Complete loss of function causes embryo lethality,

which is not surprising given that in *Arabidopsis* LSM7 is encoded by a single copy gene. What is more surprising is that *LSM7* knock-down plants are extremely temperature sensitive and unable to survive even to a moderate increase in ambient temperature from 23°C to 27°C. This extreme temperature sensitivity distinguishes *lsm7-2* from mutations in another subunit of the LSM ring, LSM5. *lsm5/sad1* mutants have been reported to be able to withstand much higher temperatures than *lsm7-2*, but perish when exposed to unphysiological temperature of 42°C[11]. To the best of our knowledge, *lsm7-2* is the only mutant that exhibits such severe temperature sensitivity and dies at a moderately increased ambient temperature of 27°C. Our results emphasise the importance of co- and post-transcriptional RNA processing in plant ambient temperature acclimation. While seedling lethality at elevated temperature is the most prominent phenotype of *lsm7-2*, the mutant displays pleiotropic defects also at lower ambient temperatures between 16°C to 23°C. The pleiotropic nature of the *lsm7-2* phenotype highlights a general problem when working with mutants affected by essential cellular machinery such as the spliceosome and/or the NMD pathway.

One way forward is to focus on a particular trait, as we have done in analysing the flowering time in *lsm7-2*. At the molecular level, early flowering in *lsm7-2* is associated with increased expression of the flowering time integrator genes *FT* and *SOC1*. This is similar to what Huertas et al. (2019)[23] reported for the *sme1*/*pcp1* mutant, which also displayed an early flowering phenotype and elevated expression of both *FT* and *SOC1*. Another commonality between *lsm7-2* and *sme1*/*pcp1* is the downregulation of *FLC* and *COOLAIR class II* transcripts. Albeit LSM7 and SME/PCP are part of different spliceosomal protein complexes, they nevertheless converge on and participate in the regulation of common downstream genes and pathways. It will be interesting to see if this pattern holds as more and more mutants in core spliceosome genes become available, or if *lsm7-2* and *sme1/pcp1* are an exception. In this context, it is important to note that even though *FLC* is downregulated in both *lsm7-2* and *sme1/pcp1*, DAS of autonomous pathway genes, such as *FLD* and *FLK*, important upstream regulators of *FLC*, has not been reported in *sme1/pcp1.* This suggests that even though LSM7 and SME/PCP might converge on the same targets, the means by which mutations in these core spliceosome genes affect *FLC* expression might nevertheless be different. Although *lsm7-2* is an AS-NMD mutant, we could not correlate *FLC* low expression in the mutant to changes in its mRNA stability or to an alternative or impaired splicing of *FLC* gene. The absence of altered RNA degradation indicates that in the l*sm7-2 FLC* is not a direct target of NMD.

An alternative to studying specific aspects of a pleiotropic phenotype, as we have done in the case of flowering time regulation, is to perform analyses at the system level. Here we combined transcriptomic and metabolomic analyses to identify molecular pathways involved in translating RNA processing defects in *lsm7-2* into a phenotype. Transcriptome and GO analyses revealed that *lsm7-2* affected a range of different biological processes. However,

GO categories related to the phytohormone auxin stood out as they were consistently overrepresented in all our analyses. Free auxin (IAA) regulates plant growth and development by controlling the fundamental processes of cell division, expansion, and differentiation. However, while IAA in low concentrations stimulates growth and development, higher concentrations can be deleterious to the plant (reviewed in [27]). To maintain auxin homeostasis, plants need to coordinate auxin synthesis, conjugation, and degradation.

Our metabolite data indicate that levels of free IAA are only moderately higher in *lsm7-2* than in wildtype, whereas precursors such as IAM and IAN, and even more so auxin conjugates such as IAA-Ala, IAA-Glu and IAA-Asp are strongly induced. The latter correlates well with the marked upregulation of *GH3s* genes, which catalyse the conjugation of IAA with amino acids for inactivation and storage. Furthermore, the finding that products of IAA oxidation such as oxIAA and oxIAA-Glc are also significantly accumulated supports our hypothesis that *lsm7-2* promotes IAA storage and inactivation to prevent overaccumulation of bioactive IAA[28]. The downregulation and upregulation of genes involved in IAA influx and efflux, respectively, are also consistent with this hypothesis.

Despite all these compensatory mechanisms, auxin homeostasis is clearly perturbed in *lsm7-2*, which in conjunction with disturbed auxin signalling, partially explains the growth defects observed in the mutant. Importantly, these defects cannot be attributed to individual auxin signalling factors. Instead, *lsm7-2* appears to cause the misregulation of a large fraction of the *AUX/*IAA, *ARF*, and *SAUR* genes encoded in the *Arabidopsis* genome. Aux/IAA proteins play a crucial role in repressing the transcription of ARF target genes in the absence of auxin[29], and are known to regulate each other's expression in intricate feedback regulation[30]. Interestingly, although expression of most *Aux/IAAs* does not change or is induced at 23°C and 16°C, *IAA6*, *IAA19,* and *IAA29* are significantly repressed specifically at 27°C, which could result in the deregulation of auxin responses, particularly in warm ambient temperatures.

More interestingly, we observed a massive downregulation of *SAUR* genes in *lsm7-2*. SAUR proteins have mainly been implicated in the regulation of plant growth via induction of cell elongation[31], although some of these genes may also participate in other processes such as in leaf senescence or cell division (reviewed in [26]). Franklin *et al.* (2011)[32] reported that high ambient temperature induces the expression of several *SAUR* genes (*SAUR19-24* and *SAUR61-68*), that participate in hypocotyl elongation and ultimately thermomorphogenesis. Interestingly, all of these SAUR genes, among others, are downregulated in *lsm7-2* at 27°C, suggesting that the mutant fails to induce thermomorphogenesis, which in turn might explain the seedling lethal phenotype at this temperature. In addition, it is well known that disturbed auxin homeostasis and signalling activate stress response pathways[33], many of which are deregulated in *lsm7-2*, thereby affecting growth and development indirectly.

Our results suggest that LSM7 is required for the correct RNA expression and processing of numerous auxin-related genes, from auxin biosynthesis to signalling and transport, thereby coordinating the response of plants to ambient temperature. We propose that the misregulation of auxin genes, and especially the downregulation of numerous *SAUR* genes, disrupts auxin homeostasis and signalling and contributes to the *lsm7-2* phenotypes, particularly at 27°C, where disruption of auxin-mediated thermomorphogenesis causes seedlings to die. Taken together, our study provides valuable insights into the role of a basal component of the splicing and RNA degradation machinery, LSM7, in responding to small changes in ambient temperature.

Methods

Plant material, growth conditions, and ambient temperature phenotyping

All genotypes used in this research were in Columbia background and mutants were obtained from Nottingham *Arabidopsis* Stock Center (NASC), *lsm7-2* (SALK_065217 or N565217) and *lsm7-1* (SALK_066076C or N677766) (**Supplementary Table 4)**. Seeds were surface sterilised with ethanol 70% and stratified at 4°C in the dark for 72 h before being sown on soil or plates. Plants were grown in long-day conditions (LD), 16h light/8h dark, in Percival chambers equipped with full range LED illumination at an intensity of 120-150µmol*$m^{-2}s^{-1}$, with controlled humidity (RH 70%) at different ambient temperatures (16°C, 23°C and 27°C) as specified in the text. Drought (25% PEG) and salt (100/200 mM NaCl) treatments were conducted on seven-day-old seedlings grown on ½ MS medium[34].

Microscopic analysis of embryos

Immature seeds were dissected by hand and cleared in Hoyer's solution (7.5g gum arabic, 5 mL glycerol, 100 g chloral hydrate and 30 mL water, diluted 2:1 with 10% (w/v) gum arabic solution) as described previously[35]. Three days after incubation, differential interference contrast (DIC) images were taken with a Zeiss Axio Imager equipped with AxioCam HRc camera.

Protein-protein interactions

The coding sequence of *LSM5* (*AT5G48870*), L*SM7* (*AT2G03870*) and its truncated form *LSM7-1t*, *PCP* (*AT2G18740*), and *PCP-like* (*AT4G30330*) were cloned into the modified yeast vectors pGADT7 or pGBKT7[36]. Oligos used in the cloning are listed in **Supplementary Table 4**. The yeast strain AH109 was used in the yeast two-hybrid assays. Transformants and interactions were screened on SD-glu medium lacking leucine (-L), tryptophan (-W), and histidine (-H). A positive interaction results in the activation of auxotrophic marker genes inside

the yeast nucleus and the growth of yeast in the selective media. Auto-activation was determined for all bait vectors to exclude false positive interactions.

Plasmid construction and plant transformation

The overexpression and rescue lines were created using the GreenGate system[37]. The coding region or genomic region of *LSM7* was amplified from Col-0 seedlings cDNA (*cLSM7*) or genomic DNA (*gLSM7*) and cloned into the GreenGate module C entry vector. For overexpression lines, the final GreenGate reaction was performed using the *35S* promoter as A module, empty B module, the C module carrying the *cLSM7*, empty D module, *rbcS* terminator in module E, and BASTA resistance as a selection marker in F module. For rescue lines, the promoter (2140 bp upstream of the start codon) and terminator (256 bp downstream of the stop codon) regions of *LSM7* were amplified from Col-0 seedlings gDNA and cloned in A module (*pLSM7*), and E module (*tLSM*), respectively. The *cLSM7* or *gLSM7* in the C module were assembled with *pLSM7* in the A module, empty B module, empty D module, *tLSM7* in the E module, and BASTA resistance as a selection marker in the F module. All the GreenGate assemblies used pGGZ003 as a destination vector. For overexpression lines, *A. thaliana* Col-0 grown at 23°C were transformed by floral dipping using Agrobacterium tumefaciens-mediated gene transfer[38], and for the rescue lines, *lsm7-2* or *lsm7-1* mutants were transformed by the same method. Transformants were selected by BASTA application. The constructs are listed in **Supplementary Table 5**.

Histological techniques and microscopy

For visualisation of the fluorescent proteins in embryos, ovules were removed from valves of siliques collected on plants grown for five weeks at 23°C. Ovules were gently squeezed to collect the embryos, then immediately used for imaging at the epifluorescence microscope Leica DMi8. For the visualisation of meristem organisation and fluorescent proteins in seedlings, a modified protocol of ClearSee was used[39,40]. Polysaccharide cell walls were stained with 0.1% calcofluor white M2R[40]. Confocal laser scanning microscopy experiments were performed in an LSM780 or LSM880 microscope (Zeiss). Combinatorial fluorescence analysis was run as sequential scans. The following excitation and emission settings were used: EGFP, 488/500 to 550 nm; calcofluor white, 405/425 to 475 nm and Hoechst 33342, 430/480 to 405 nm.

LSM7 subcellular quantification

pLSM7::LSM7::GFP lsm7-2 rescue seedling grown for 9 days at 23°C were shifted for 24h to 16°C or 27°C, or kept at 23°C as control, time after which were live imaged. To determine LSM7-GFP enrichment in the nucleus, 10-day-old rescue seedlings were counterstained* in

ClearSee with 10 µg/mL Hoechst 33342 for 1 day[39]. In order to reduce exposing cells to any other factor than the temperature treatment, LSM7-GFP observations were performed in seedlings mounted in water right after taking them out of incubators. Imaging of epidermal cells in the root tip was recorded in z-plane stacks. For measurements, optical stack slices in a 5µM-thick section, spaced 1µM between each other, were converted into a maximum projection file, in 8-bit depth. Mean intensity was quantified in regions of interest (ROI) in the nucleus and cytoplasm ranging between 1 and 2 μm^2. The mean intensity, which is the average fluorescence per area unit, was calculated by adding the fluorescence intensity (in a 8-bit scale of 0 to 255) of each pixel in an area, divided by the number of pixels in that area. At least two cells showing clearly visible nuclei were considered per stack file, having each cell associated with a ROI in the nucleus and another to the cytoplasm. The mean intensity of measurements of different pictures were analysed together. Images were processed and analysed using the Fiji package of ImageJ (https://fiji.sc).

Immunoblot analysis

For LSM7 protein expression, nine days old *lsm7-2* and Col-0 seedlings bearing the *pLSM7:GFP:gLSM7:tLSM7* construct were grown at 23°C in LD conditions and shifted to 16°C or 27°C, or kept at 23°C for 24h. Samples were collected at ZT6, and total proteins were extracted with the TCA/Acetone method. Proteins were resolved in 4-15% pre-cast SDS-PAGE (Biorad cat nº 4561085) at 80V for two hours and transferred to PVDF membrane (Immobilon-P; Millipore) for immunoblot analysis. Two identical gels and relative membranes were made at the same time for the detection of GFP-LSM7 and tubulin (loading control). First, the membranes were blocked with 3% BSA in PBS for two hours. Then, one membrane was incubated with anti-GFP antibody (1/4000 Abcam cat. nº Ab290) with 3% BSA in PBS and the other with anti-Tubulin (1/10000 Agrisera cat. nº AS10-680) in 3% skimmed milk in PBS for two hours at room temperature. Both membranes were washed with TBS-T (Tween 20; 50-mM Tris, 150-mM NaCl, and 0.05% [v/v] Tween 20) three times and incubated with the anti-rabbit IgG-HRP antibody (1/20,000, Agrisera cat. nº AS10-1014) in 3% w/v BSA (anti-GFP) or 3% milk (anti-tubulin) in PBS for two hours. After three washes with TBS-T, the membranes were incubated with Chemiluminescent Substrate (Amersham cat. nº RPN2232) for 1 min. Proteins were visualised with the Azure Imaging System (Azure Biosystems, Inc).

Transcriptomics and bioinformatics analysis

To analyse variation in splicing patterns in response to a change in temperature, plants were grown for nine days at 23°C in LD conditions and shifted to 16°C, 27°C or kept at 23°C in LD, for 3h or 24h. Three pools of ten seedlings' aerial parts for each line in each temperature were

collected after the shift at ZT6 in liquid nitrogen. Frozen samples were ground to a fine powder, and total RNA was extracted with Qiagen Plant RNeasy kit according to the manufacturer's instructions and treated with DNAseI (Thermo Scientific). RNA concentrations and integrity were determined using Qubit RNA kit (Thermo Scientific) and Bioanalyser RNA Nano kit (Agilent). Strand-specific mRNA-Seq was conducted by Novogene using NEB Next® Ultra RNA Library Prep Kit for Illumina. Briefly, mRNA was purified from total RNA using poly-T oligo-attached magnetic beads. After fragmentation, the first-strand cDNA was synthesised using random hexamer primers followed by the second-strand cDNA synthesis, followed by repair, A-tailing, adapter ligation, and size selection. After amplification and purification, the insert size of the library was validated on an Agilent 2100 and quantified using quantitative PCR (qPCR). Libraries were then sequenced on Illumina NovaSeq 6000 S4 flowcell with PE150. The data analysis was conducted using R and Bioconductor with some modifications. The quality of the sequences was confirmed using Trimmomatic[42] and FastQC. Reads were mapped to the ATRTD2-QUASI transcriptome annotation[43] using Salmon[44]. After normalisation, the profiles of the samples were assessed by principal component analysis (PCA). Differentially expressed (DE) genes between temperatures and genotypes across the time points were identified at each time point using limma-voom likelihood ratio tests after negative binomial fittings using the package in the 3D pipeline[45]. Genes with False Discovery Rate (FDR)-corrected-values ≤ 0.05 and fold-change (log2) threshold of 0.5 were classified as differentially expressed (**Supplementary Tables 2 and 3**). To identify processes potentially involved in the plant response to the different temperatures at the different time points, GO Enrichment Analysis was performed using online David software version 2021[46] (**Supplementary Table 4**).

Expression analysis by quantitative real-time PCR (qPCR)

RNA samples were treated with DNaseI RNase-free (Thermo Scientific) for 30 min at 37°C to remove DNA contamination and retro-transcribed with RevertAid First Strand cDNA Synthesis kit (Thermo Fisher) in accordance with the manufacturer's instructions. Primers were designed with Primer 3 software[47] using as criterion amplified products from 80 to 180 bp with a Tm of 60 ± 1°C (primer sequences are listed in **Supplementary Table 5**). Both target and reference genes were amplified from cDNA. cDNA samples were used in qPCR reactions with LightCycler Sybr (Roche), using CFX96 Real-time System (Biorad). The relative expressions were calculated through a normalised expression ratio using an efficiency-(E)-calibrated model with the experimental significance was estimated through 2000 randomisations of Cq data in each experimental comparison using REST software (version mcs) (http://rest.gene-quantification.info/). Three technical and three biological replicates were performed for each sample.

RNA half-life determination

Col-0 and *lsm7-2* seedlings were grown for nine days on vertical plates containing ½ MS medium 1% agar pH 5.7, then transferred to a six-well-plate containing incubation buffer (1 mM PIPES pH 6.25, 1 mM trisodium citrate, 1 mM KCl, 15 mM sucrose). After 30 min of incubation, cordycepin (3'deoxyadenosine, Sigma-Aldrich) was added to a final concentration of 150 mg/L and internalised using a vacuum pump (two cycles of 5 min). Seedlings were collected at 0, 15, 30, 45, 60, and 90 min and frozen in liquid nitrogen. To estimate RNA half-lives of *FLC* and *COOLAIR II* RNAs, total RNA was isolated using Trizol (Thermo Fisher), treated with Turbo DNAse (Thermo Fisher), reverse transcribed, and gene expression analysed by RT-qPCR (as described in the previous section). Short- and long-lived transcripts *EXPANSIN-LIKE1* (*Expansin L1*) and *Eukaryotic translation initiation factor 4A1* (*EIF4A1A*) were used as unstable and stable controls, respectively. Ct-values were normalised by the Ct-value at time point 0 [Ct(n) = (ln(Ct/Ct(0))*(-10)] and plotted as degradation curves. Slopes of the curves were used to calculate RNA half-lives [t1/2 = (ln2)/slope] as described by Jia *et al*.,[48]. Primers are listed in **Supplementary Table 5**.

IAA and IAA-conjugate measurements

Seedlings of *lsm7-2* and *Col-0* were grown for nine days at 23°C in LD conditions and then shifted to 16°C or 27°C or kept at 23°C for 24 h. Five pools of 20 mg seedling' shoots for each genotype at each temperature were collected at ZT6 in liquid nitrogen. The extraction, purification, and LC-MS analysis of endogenous IAA, its precursors, and metabolites were carried out according to Novák and collaborators[49]. A bead mill (27 Hz, 10 min, 4°C; MixerMill, Retsch GmbH, Haan, Germany) was used to homogenise 20 mg of frozen material per sample, which was then extracted in 1 ml of 50 mM sodium phosphate buffer containing 1% sodium diethyldithiocarbamate and a mixture of $^{13}C_6$- or deuterium-labelled internal standards. After centrifugation (14 000 RPM, 15 min, 4°C), the supernatant was divided into two aliquots. The first aliquot was derivatised using cysteamine (0.25 M; pH 8; 1 h; room temperature; Sigma-Aldrich); the second aliquot was immediately further processed as follows: the pH of the sample was adjusted to 2.5 by 1 M HCl and applied on a preconditioned solid-phase extraction column, Oasis HLB (30 mg 1 cc, Waters Inc., Milford, MA, USA). After sample application, the column was rinsed with 2 ml of 5% methanol. The compounds of interest were then eluted with 2 ml of 80% methanol. The derivatised fraction was similarly purified. Mass spectrometry analysis and quantification were performed by an LC-MS/MS system comprising a 1290 Infinity Binary LC System coupled to a 6490 Triple Quad LC/MS System with Jet Stream and Dual Ion Funnel technologies (Agilent Technologies, Santa Clara, CA, USA).

Statistical information

Microsoft Excel and R Studio were used for statistical analysis (Rv4.0.2). Statistical information is included in figures and figure legends (P-value, P-value levels, and sample number). For the RNA-seq analysis, the FDR-corrected values prevented significance. P-value levels are indicated on the figures by asterisks as follows: * ($p<0.05$), ** ($p<0.01$), *** ($p<0.001$).

Code availability

The code used for the RNA-seq analysis is available in the GitHub public repository: https://github.com/snardeli/Nardeli_et_al_2023.

Data availability

The RNA-seq data generated in this study have been deposited at the European Nucleotide Archive (ENA, https://www.ebi.ac.uk/ena) under the accession number XXX. Lists of differentially expressed genes and transcripts are made available as Supplementary Files. Other data that support the findings of this study are available from the corresponding author upon request.

References

1. Exposito-Alonso, M. Seasonal timing adaptation across the geographic range of Arabidopsis thaliana. *Proceedings of the National Academy of Sciences of the United States of America* vol. 117 9665–9667 (2020).
2. Calixto, C. P. G. *et al.* Rapid and Dynamic Alternative Splicing Impacts the Arabidopsis Cold Response Transcriptome. *Plant Cell* **30**, 1424–1444 (2018).
3. Lekontseva, N. V., Stolboushkina, E. A. & Nikulin, A. D. Diversity of LSM Family Proteins: Similarities and Differences. *Biochemistry* **86**, S38–S49 (2021).
4. He, W. & Parker, R. Functions of Lsm proteins in mRNA degradation and splicing. *Curr. Opin. Cell Biol.* **12**, 346–350 (2000).
5. Wu, D. *et al.* Lsm2 and Lsm3 bridge the interaction of the Lsm1-7 complex with Pat1 for decapping activation. *Cell Res.* **24**, 233–246 (2014).
6. Arribas-Layton, M., Wu, D., Lykke-Andersen, J. & Song, H. Structural and functional control of the eukaryotic mRNA decapping machinery. *Biochim. Biophys. Acta* **1829**, 580–589 (2013).
7. Kurosaki, T., Popp, M. W. & Maquat, L. E. Quality and quantity control of gene expression by nonsense-mediated mRNA decay. *Nat. Rev. Mol. Cell Biol.* **20**, 406–420 (2019).
8. Dikaya, V. *et al.* Insights into the role of alternative splicing in plant temperature response. *J. Exp. Bot.* (2021) doi:10.1093/jxb/erab234.
9. Mateos, J. L. *et al.* PICLN modulates alternative splicing and light/temperature responses in plants. *Plant Physiol.* (2022) doi:10.1093/plphys/kiac527.
10. Perea-Resa, C., Hernández-Verdeja, T., López-Cobollo, R., del Mar Castellano, M. & Salinas, J. LSM proteins provide accurate splicing and decay of selected transcripts to ensure normal Arabidopsis development. *Plant Cell* **24**, 4930–4947 (2012).
11. Okamoto, M. *et al.* Sm-Like Protein-Mediated RNA Metabolism Is Required for Heat Stress Tolerance in Arabidopsis. *Front. Plant Sci.* **7**, 1079 (2016).
12. Esteve-Bruna, D. *et al.* Prefoldins contribute to maintaining the levels of the spliceosome LSM2-8 complex through Hsp90 in Arabidopsis. *Nucleic Acids Res.* **48**, 6280–6293 (2020).
13. Capovilla, G. *et al.* PORCUPINE regulates development in response to temperature through alternative splicing. *Nat Plants* **4**, 534–539 (2018).
14. Meinke, D. W. Genome-wide identification of EMBRYO-DEFECTIVE (EMB) genes required for growth and development in Arabidopsis. *New Phytol.* **226**, 306–325 (2020).
15. Verma, S., Attuluri, V. P. S. & Robert, H. S. An Essential Function for Auxin in Embryo Development. *Cold Spring Harb. Perspect. Biol.* **13**, (2021).
16. Friml, J. *et al.* Efflux-dependent auxin gradients establish the apical-basal axis of

Arabidopsis. *Nature* **426**, 147–153 (2003).

17. Hu, Y. *et al.* Cell kinetics of auxin transport and activity in Arabidopsis root growth and skewing. *Nat. Commun.* **12**, 1657 (2021).
18. Mazur, E., Kulik, I., Hajný, J. & Friml, J. Auxin canalization and vascular tissue formation by TIR1/AFB-mediated auxin signaling in Arabidopsis. *New Phytol.* **226**, 1375–1383 (2020).
19. Aloni, R., Aloni, E., Langhans, M. & Ullrich, C. I. Role of auxin in regulating Arabidopsis flower development. *Planta* **223**, 315–328 (2006).
20. Kazan, K. Auxin and the integration of environmental signals into plant root development. *Ann. Bot.* **112**, 1655–1665 (2013).
21. Shibasaki, K., Uemura, M., Tsurumi, S. & Rahman, A. Auxin response in Arabidopsis under cold stress: underlying molecular mechanisms. *Plant Cell* **21**, 3823–3838 (2009).
22. Quint, M. *et al.* Molecular and genetic control of plant thermomorphogenesis. *Nat Plants* **2**, 15190 (2016).
23. Huertas, R. *et al.* Arabidopsis SME1 Regulates Plant Development and Response to Abiotic Stress by Determining Spliceosome Activity Specificity. *Plant Cell* **31**, 537–554 (2019).
24. Orchard, S. *et al.* The MIntAct project--IntAct as a common curation platform for 11 molecular interaction databases. *Nucleic Acids Res.* **42**, D358–63 (2014).
25. Burko, Y. *et al.* PIF7 is a master regulator of thermomorphogenesis in shade. *Nat. Commun.* **13**, 4942 (2022).
26. Stortenbeker, N. & Bemer, M. The SAUR gene family: the plant's toolbox for adaptation of growth and development. *J. Exp. Bot.* **70**, 17–27 (2019).
27. Woodward, A. W. & Bartel, B. Auxin: regulation, action, and interaction. *Ann. Bot.* **95**, 707–735 (2005).
28. Jez, J. M. Connecting primary and specialized metabolism: Amino acid conjugation of phytohormones by GRETCHEN HAGEN 3 (GH3) acyl acid amido synthetases. *Curr. Opin. Plant Biol.* **66**, 102194 (2022).
29. Li, H., Cheng, Y., Murphy, A., Hagen, G. & Guilfoyle, T. J. Constitutive repression and activation of auxin signaling in Arabidopsis. *Plant Physiol.* **149**, 1277–1288 (2009).
30. Hagen, G. & Guilfoyle, T. Auxin-responsive gene expression: genes, promoters and regulatory factors. *Plant Mol. Biol.* **49**, 373–385 (2002).
31. Ren, H., Park, M. Y., Spartz, A. K., Wong, J. H. & Gray, W. M. A subset of plasma membrane-localized PP2C.D phosphatases negatively regulate SAUR-mediated cell expansion in Arabidopsis. *PLoS Genet.* **14**, e1007455 (2018).
32. Franklin, K. A. *et al.* Phytochrome-interacting factor 4 (PIF4) regulates auxin biosynthesis at high temperature. *Proc. Natl. Acad. Sci. U. S. A.* **108**, 20231–20235 (2011).

33. Saini, K. *et al.* Alteration in Auxin Homeostasis and Signaling by Overexpression Of PINOID Kinase Causes Leaf Growth Defects in Arabidopsis thaliana. *Front. Plant Sci.* **8**, 1009 (2017).
34. Verslues, P. E., Agarwal, M., Katiyar-Agarwal, S., Zhu, J. & Zhu, J.-K. Methods and concepts in quantifying resistance to drought, salt and freezing, abiotic stresses that affect plant water status. *Plant J.* **45**, 523–539 (2006).
35. Bayer, M. *et al.* Paternal control of embryonic patterning in Arabidopsis thaliana. *Science* **323**, 1485–1488 (2009).
36. Zacharaki, V. *et al.* Impaired KIN10 function restores developmental defects in the Arabidopsis trehalose 6-phosphate synthase1 (tps1) mutant. *New Phytol.* **235**, 220–233 (2022).
37. Lampropoulos, A. *et al.* GreenGate---a novel, versatile, and efficient cloning system for plant transgenesis. *PLoS One* **8**, e83043 (2013).
38. Clough, S. J. & Bent, A. F. Floral dip: a simplified method for Agrobacterium-mediated transformation of Arabidopsis thaliana. *Plant J.* **16**, 735–743 (1998).
39. Kurihara, D., Mizuta, Y., Sato, Y. & Higashiyama, T. ClearSee: a rapid optical clearing reagent for whole-plant fluorescence imaging. *Development* **142**, 4168–4179 (2015).
40. Ursache, R., Andersen, T. G., Marhavý, P. & Geldner, N. A protocol for combining fluorescent proteins with histological stains for diverse cell wall components. *Plant J.* **93**, 399–412 (2018).
41. Hacham, Y. *et al.* Brassinosteroid perception in the epidermis controls root meristem size. *Development* **138**, 839–848 (2011).
42. Bolger, A. M., Lohse, M. & Usadel, B. Trimmomatic: A flexible trimmer for Illumina sequence data. *Bioinformatics* **30**, 2114–2120 (2014).
43. Zhang, R. *et al.* A high quality Arabidopsis transcriptome for accurate transcript-level analysis of alternative splicing. *Nucleic Acids Res.* **45**, 5061–5073 (2017).
44. Patro, R., Duggal, G., Love, M. I., Irizarry, R. A. & Kingsford, C. Salmon provides fast and bias-aware quantification of transcript expression. *Nat. Methods* **14**, 417–419 (2017).
45. Guo, W. *et al.* 3D RNA-seq: a powerful and flexible tool for rapid and accurate differential expression and alternative splicing analysis of RNA-seq data for biologists. *RNA Biol.* 1–14 (2020).
46. Huang, D. W., Sherman, B. T. & Lempicki, R. A. Systematic and integrative analysis of large gene lists using DAVID bioinformatics resources. *Nat. Protoc.* **4**, 44–57 (2009).
47. Rozen, S. & Skaletsky, H. Primer3 on the WWW for general users and for biologist programmers. *Methods Mol. Biol.* **132**, 365–386 (2000).
48. Jia, T. *et al.* The Arabidopsis MOS4-Associated Complex Promotes MicroRNA Biogenesis and Precursor Messenger RNA Splicing. *Plant Cell* **29**, 2626–2643 (2017).

49. Novák, O. *et al.* Tissue-specific profiling of the Arabidopsis thaliana auxin metabolome. *Plant J.* **72**, 523–536 (2012).

Acknowledgements

The authors acknowledge the facilities and technical assistance of the Umeå Plant Science centre. More in particular, we would like to thank Dr. Nicolas Delhomme and the UPSCb Bioinformatics facility (https://www.upsc.se/platforms/upsc-bioinformatics-facility.html) for the bioinformatics support; the personnel working at the Microscopy facility (https://www.upsc.se/platforms/microscopy-facility.html); Dr Jan Šimura and the Swedish Metabolomics Center (www.swedishmetabolomicscentre.se) for carrying out the auxin metabolites' analysis; Dr Shiv Meena for discussions related to the cordycepin assay, and all members of the MS group for the scientific discussions. This work was supported by the German Research Foundation (Deutsche Forschungsgemeinschaft - DFG) (BA3356/3-1, BA3356/4-1, and SFB1101/B12) to MB and, the Knut and Alice Wallenberg Foundation (KAW 2018.0202) to MS.

Author contributions

SMN, VZ, SC, MS, and DG designed the experiments. SMN and DG created the lines, phenotyped the plants, and performed the RNA-seq, qPCR and cordycepin experiments, with the contribution of VZ. NR-M and DG performed the Col-0 and microscopy experiments. KY and MB performed microscopy analyses on the embryos. SC performed the immunoblot assays. SMN performed the interactome assays. SMN analysed the RNA-seq with the contribution of VZ and DG. SMN and VZ analysed the auxin data. SMN and DG wrote the manuscript with contributions from all authors.

Competing interests

The authors declare no competing interests.

Materials & correspondence

Correspondence to MS (markus.schmid@slu.se).

Main Figures & Figure Legends

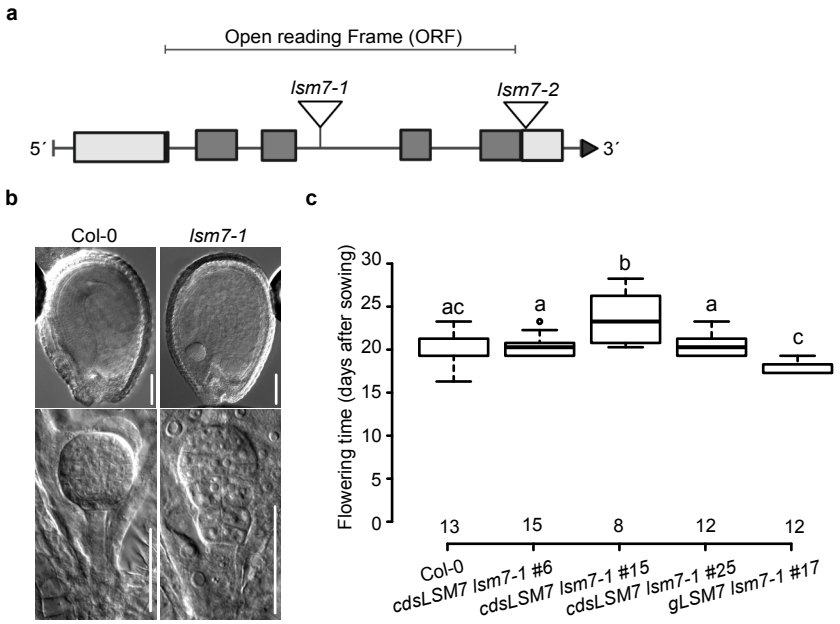

Figure 1. *lsm7-1* knock-out mutant is embryo lethal. a Scheme of the *LSM7* gene and the T-DNA mutants used in this study. Dark grey boxes represent exons, light grey boxes are UTRs, and lines are introns. Inverted triangles indicate T-DNA insertions. **b** Wildtype and *lsm7-1-/-* embryos collected from *lsm7-1+/-* plants grown at different temperatures. Photos were taken 36 days after sowing at 16°C and 18 days after sowing in case of plants grown at 23°C and 27°C. The scale bar is 100µm. **c** Ectopic expression of *LSM7* rescues *lsm7-1* embryo lethality. The indicated flowering time refers to the days from sowing to the emergence of visible flower buds. Data for Col-0 and different T2 lines are shown, where # represents the line numbering. Numbers on the x-axis are numbers of individuals. One-way ANOVA was used for statistical analysis. Different letters above the box plots indicate categories that are statistically different ($p \leq 0.05$).

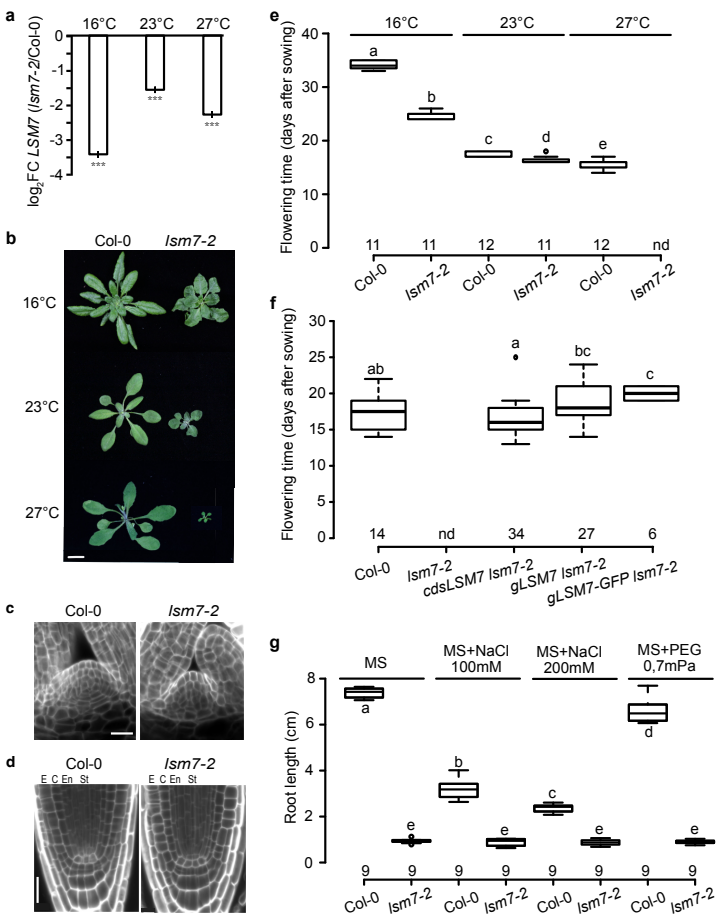

Figure 2. LSM7 is important for correct plant growth at both low and high ambient temperatures. a Relative *LSM7* expression (log_2FC) in different temperatures is shown as the ratio of *lsm7-2*/Col-0 expression values. The significance of FC values are indicated by three asterisks ($p<0.001$). **b** Phenotype of wild-type and mutant plants grown at different temperatures. Scale bar is 1 cm. **c-d** Overview of the shoot apical meristem and the cell organisation in the meristematic zone of the root tip in seven-day-old wild-type and mutant seedlings. Cell organisation is observed in median longitudinal confocal sections (scale bar is 20µM). E, Epidermis; C, Cortex; En, Endodermis; St, Stele. **e-f** The indicated flowering time refers to the days from sowing to the emergence of visible flower buds. Numbers on the x-axis are numbers of scored individuals. One-way ANOVA was used for statistical analysis. Different letters indicate categories that are statistically different ($p\leq0.05$). **e** Data refer to *lsm7-2* and Col-0 grown under different temperatures. **f** Ectopic expression of *LSM7* rescues *lsm7-2* lethality at 27°C. T1 plants expressing different constructs in *lsm7-2* background were scored at 27°C. **g** Root length (cm) of *lsm7-2* and Col-0 seedlings grown on plates under different media. MS, Murashige and Skoog; NaCl, Natrium Chloride; PEG, Polyethyleneglycol. Numbers on the x-axis are numbers of individuals. One-way ANOVA was used for statistical analysis. Different letters indicate categories that are statistically different ($p\leq0.05$).

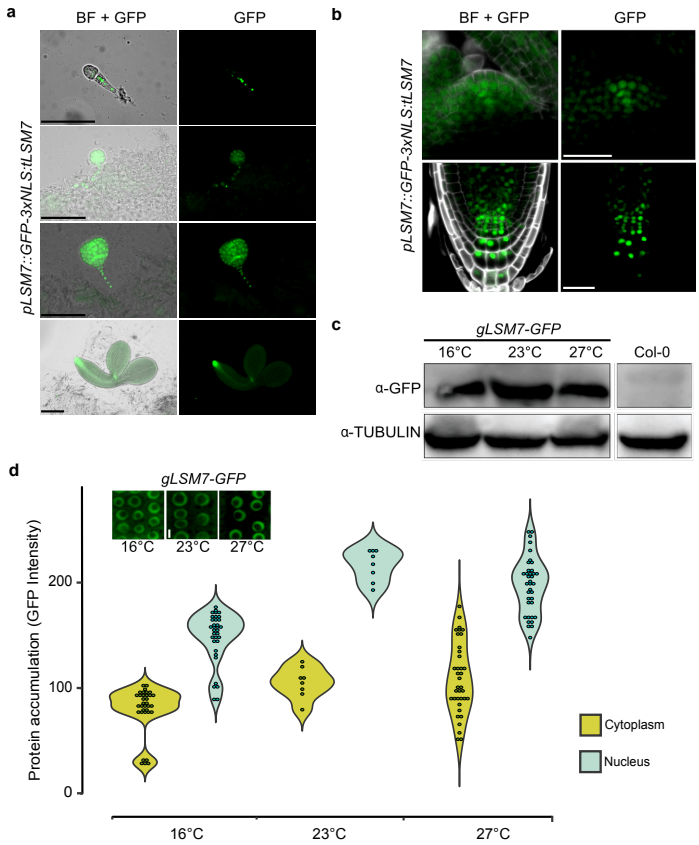

Figure 3. LSM7 distribution and stability are not affected by changes in ambient temperature. a *LSM7* promoter activity in *Arabidopsis thaliana* embryos at different developmental stages. BF, bright field. Scale bar is 30uM. **b** *LSM7* promoter activity in cells of the shoot apical meristem and root tip. BF, bright field. Scale bar is 50uM. **c** Accumulation of LSM7-GFP expressed under native promoter and terminator in plants grown under different ambient temperatures. Detection of LSM7-GFP by Western Blot using an anti-GFP antibody. Anti-TUBULIN is used as a loading control. **d** Subcellular localisation of LSM7-GFP in plants grown at different temperatures. Each dot within the violin plots represents an independent measurement. Mean intensity indicates mean fluorescence signal intensity with 8-bit depth.

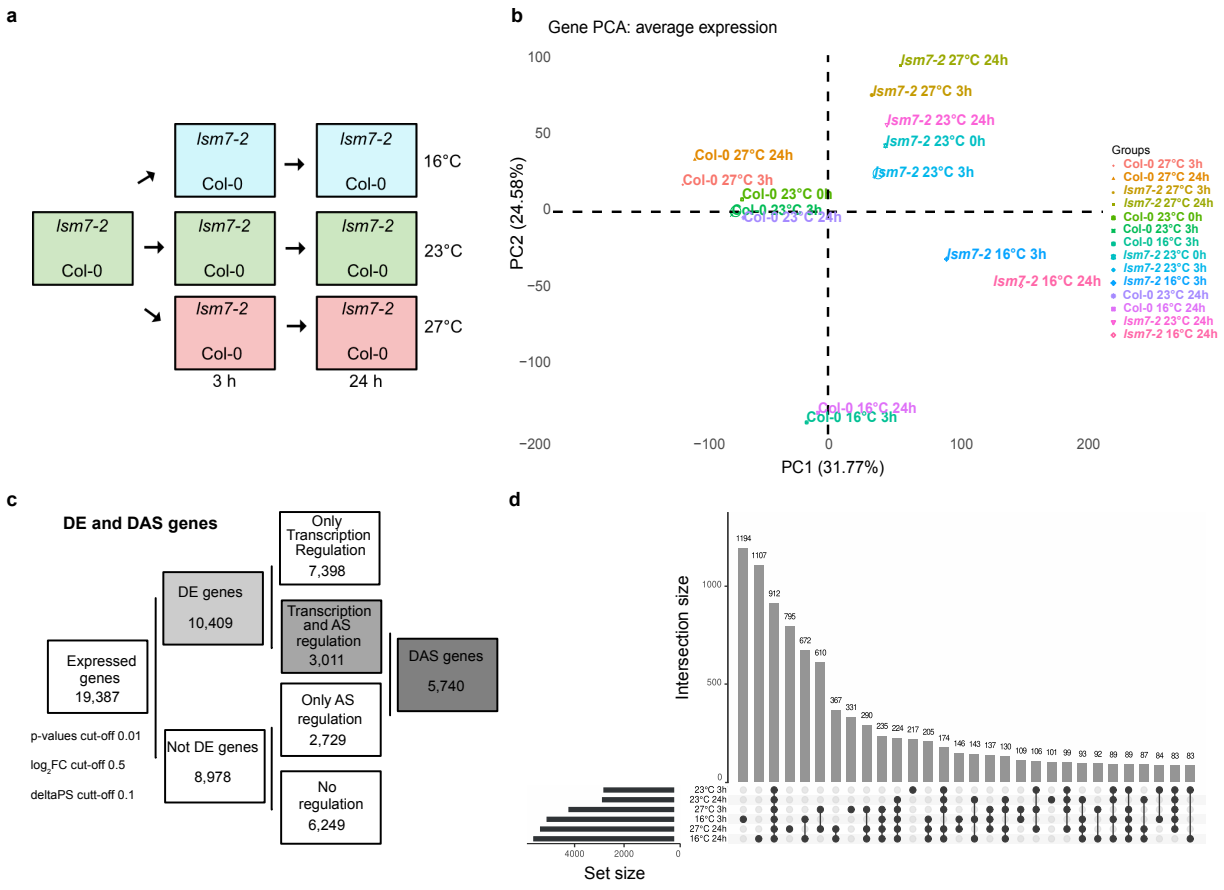

Figure 4. *lsm7-2* transcriptome upon shifts in ambient temperature. **a** RNA-seq experimental design. **b** Principal Component Analysis (PCA) for RNA-seq samples. Each data point from the RNA-seq data reflects the average gene expression (n = 3). **c N**umber of genes or transcripts that are only regulated by transcription (DE), only by alternative splicing (AS), or both transcription and alternative splicing (DAS) is shown**. d** Intersection of differentially expressed genes (DEGs; log_2FC *lsm7-2*/Col-0) of seedlings in each tested condition detected by RNA-seq is visualised using an Upset plot. The total intersection sizes are displayed above each bar, and the number of genes (set sizes) are represented by black bars.

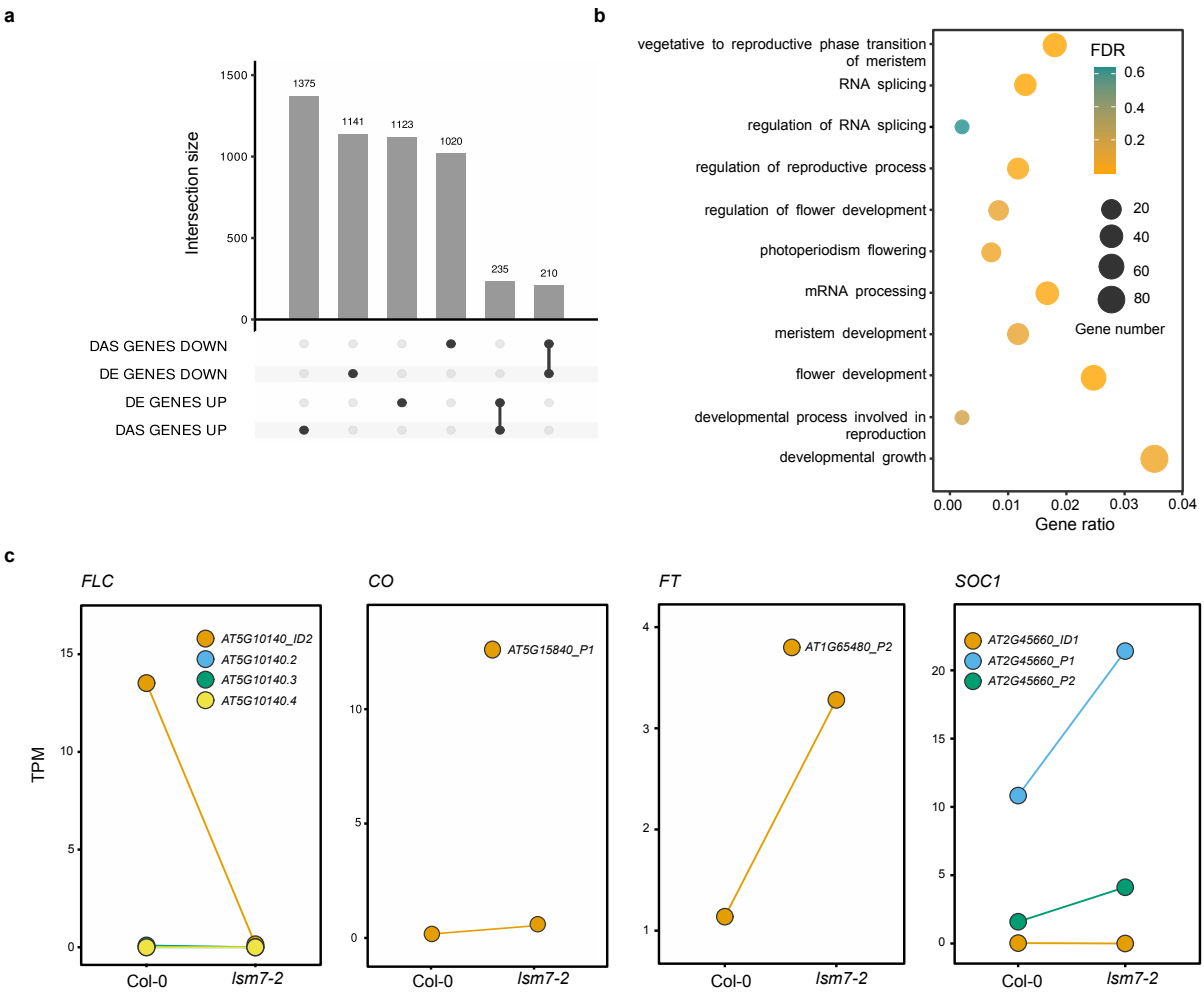

Figure 5. Downregulation of *LSM7* modulates the flowering transcriptome. a Up- or down-regulated differentially expressed genes (DEGs) and differentially alternatively spliced genes (DAS) in nine-day-old *lsm7-2* and Col-0 seedlings grown at 23°C. The intersection of DEGs (log_2FC *lsm7-2*/Col-0) of seedlings in each tested condition detected by RNA-seq is visualised using an Upset plot. Total intersection sizes are displayed in black above each bar. **b** Representative Gene Ontology (GO) terms for enriched Biological Processes (BP) for DAS genes in *lsm7-2*. The number of genes are represented by the circle sizes and the false discovery rate (FDR) by colours. **c** RNA-seq expression levels (TPM: transcripts per million) of *FLC, CO, FT* and *SOC1* in *lsm7-2* and Col-0 nine-day-old seedlings. Genes' isoform annotations were retrieved from the ATRTD2 database.

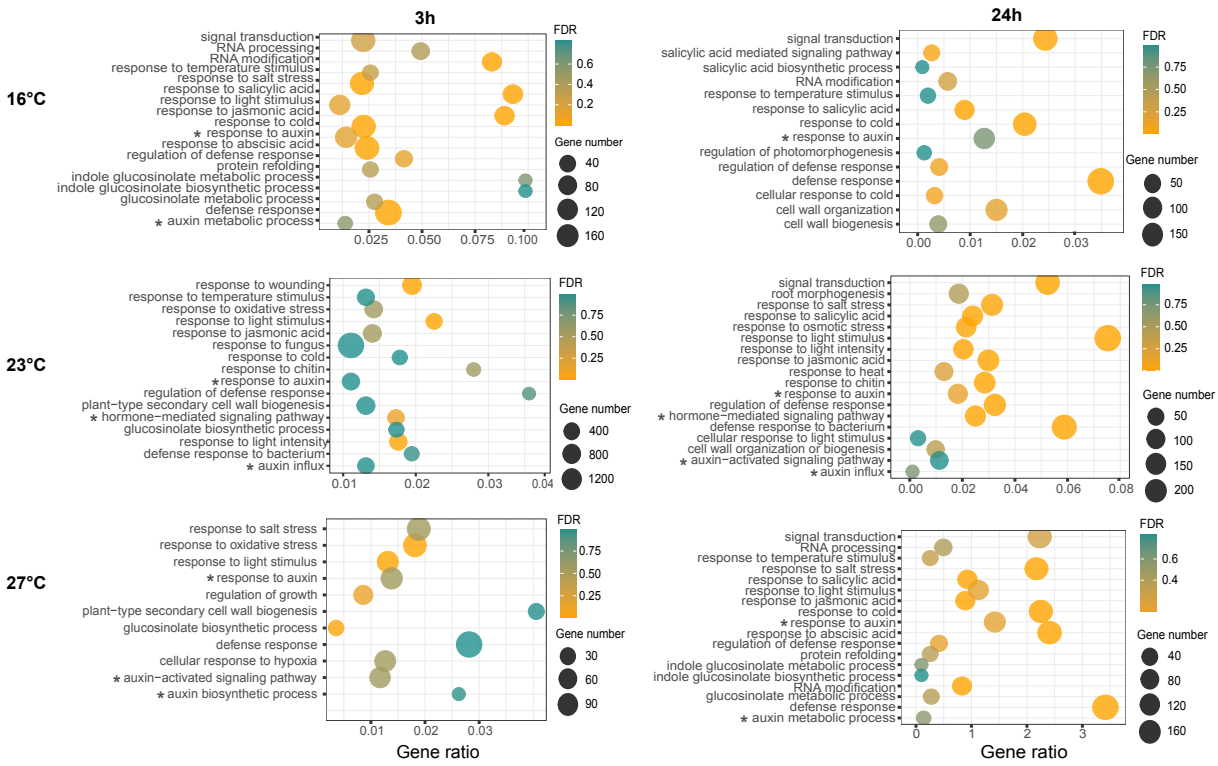

Figure 6. LSM7 participates in the regulation of many different biological processes. Selected Biological Processes (BPs) for enriched Gene Ontologies (GOs) for DEGs of *lsm7-2* compared to Col-0 of nine-day-old seedlings after initial (3h) and late (24h) exposure to different ambient temperatures (16°C, 23°C and 27°C). The number of genes are represented by the circle sizes and the false discovery rate (FDR) by colours. Stars mark auxin-related GOs.

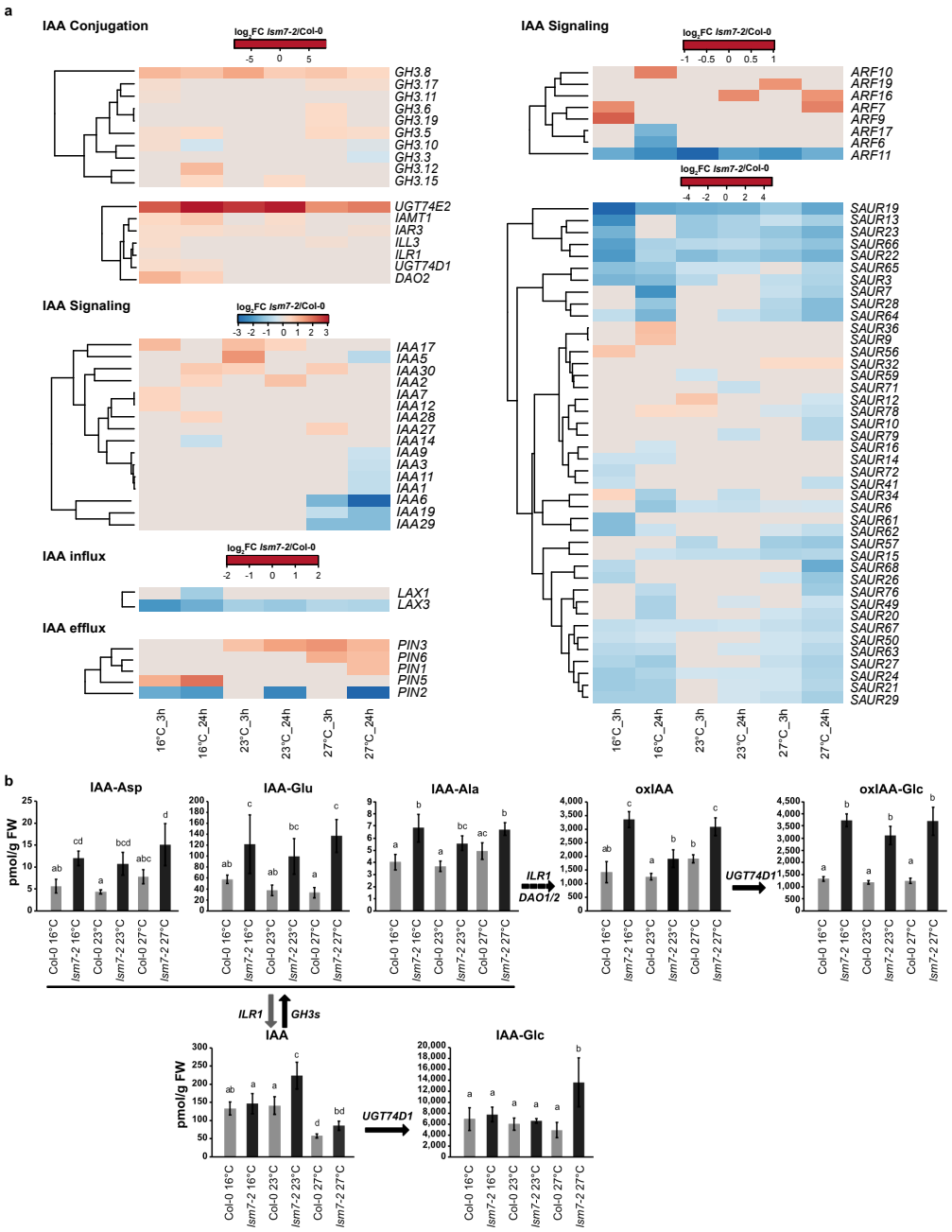

Figure 7. Auxin pathway is modulated in the *lsm7-2* mutant. a Heatmaps of significant differentially expressed auxin-responsive genes' expression ($\log_2$FC *lsm7-2*/Col-0) in seedlings exposed to different ambient temperatures, organised according to their function. Shades of red indicate up-regulated genes and shades of blue indicate down-regulated genes in *lsm7-2*. **b** Analysis of IAA and IAA metabolites under different temperatures in the *lsm7-2* mutant (dark grey) and Col-0 (light grey). Error bars represent the standard deviation (SD) of mean values from five biological replicates and letters the statistical differences among the genotypes and conditions based on ANOVA and Tukey's HSD test. Quantification is presented as pmol/gram of fresh weight (pmol/g FW). Arrows indicate the main genes involved in the step. Solid lines indicate direct reactions, dashed lines indirect reactions.